



Article

Simulation of Ni²⁺ Chelating Peptides Separation in IMAC: Prediction of Langmuir Isotherm Parameters from SPR Affinity Data

Rachel Irankunda *, Pauline Jambon, Alexandra Marc, Jairo Andrés Camaño Echavarría D, Laurence Muhr and Laetitia Canabady-Rochelle *D

Université de Lorraine, CNRS, LRGP, F-54000 Nancy, France

* Correspondence: rachel.irankunda@univ-lorraine.fr (R.I.); laetitia.canabady-rochelle@univ-lorraine.fr (L.C.-R.); Tel.: +33-(0)-372-743-886 (L.C.-R.)

Abstract: Chromatography modeling for simulation is a tool that can help to predict the separation of molecules inside the column. Knowledge of sorption isotherms in chromatography modeling is a crucial step and methods such as frontal analysis or batch are used to obtain sorption isotherm parameters, but they require a significant quantity of samples. This study aims to predict Langmuir isotherm parameters from Surface Plasmon Resonance (SPR) affinity data (requiring less quantity of sample) to simulate metal chelating peptides (MCPs) separation in Immobilized Metal ion Affinity Chromatography (IMAC), thanks to the analogy between both techniques. The validity of simulation was evaluated by comparing the peptide's simulated retention time with its experimental retention time obtained by IMAC. Results showed that the peptide affinity constant (K_A) can be conserved between SPR and IMAC. However, the maximal capacity (k_A) must be adjusted by a correction factor to overcome the geometry differences between IMAC (spherical particles) and SPR (plane sensor ship). Therefore, three approaches were studied; the best one was to use k_A 0 obtain the k_A 1 obtain the k_A 2 of the peptide, thus minimizing the discrepancy between the experimental and simulated retention times of a peptide.

Keywords: metal chelating peptides; chromatography modeling; transport dispersive model; simulation; IMAC; SPR; sorption isotherm

1. Introduction

To date, in an ecological transition context, there is a huge interest in discovering new biomolecules, as an alternative to chemicals produced by the petroleum industries. Yet, the discovery of natural biomolecules is challenged by the separation processes to recover them. Hence, peptide hydrolysates obtained from protein hydrolysis can be considered as a bank of peptides in which to screen some target peptides, endowed with various biofunctionalities and bioactivities. Some peptides present in these hydrolysates, known as metal chelating peptides (MCPs), are able to form complexes with metals and thus have a variety of industrial applications in the food, cosmetic, and health domains [1,2]. For example, MCPs can be used to inhibit lipid oxidation in oil-in-water emulsions by complexing metal ions which act as prooxidants in emulsion systems [3]. They can also be used to enhance the mineral absorption and bioavailability of zinc in the human body [4,5]. Despite the huge interest, it is still a challenge to recover and separate these MCPs from hydrolysate since they are present at very low concentrations in this complex mixture. Generally, various types of chromatography are used to separate peptides, such as ion exchange chromatography, and reverse phase-HPLC; yet, Immobilized Metal ion Affinity Chromatography (IMAC) has particularly been used to separate and purify MCPs [6–8]. Indeed, in IMAC, the separation is based on the interaction between peptides and a metal



Citation: Irankunda, R.; Jambon, P.; Marc, A.; Camaño Echavarría, J.A.; Muhr, L.; Canabady-Rochelle, L. Simulation of Ni²⁺ Chelating Peptides Separation in IMAC: Prediction of Langmuir Isotherm Parameters from SPR Affinity Data. *Processes* 2024, 12, 592. https://doi.org/10.3390/ pr12030592

Academic Editor: Cunshan Zhou

Received: 25 December 2023 Revised: 23 February 2024 Accepted: 28 February 2024 Published: 15 March 2024



Copyright: © 2024 by the authors. Licensee MDPI, Basel, Switzerland. This article is an open access article distributed under the terms and conditions of the Creative Commons Attribution (CC BY) license (https://creativecommons.org/licenses/by/4.0/).

Processes **2024**, 12, 592 2 of 19

ion, which is immobilized on a support via a complexing agent such as Nitrilotriacetic acid (NTA) or iminodiacetic acid (IDA) [9]. Thus, it is possible to choose which metal ion to immobilize in IMAC chromatography and from the Hard and Soft Acid and Base (HSAB) theory to predict the composition of peptides mostly to be complexed by the immobilized metal [10]. For example, metal chelating peptides separated in IMAC-Ni²⁺ would contain mostly histidine residues and tryptophane residues [11,12]. To date, MCPs' discovery in hydrolysate is led by several consecutive cycles of separation/bioactivity and biofunctional evaluation to identify a single sequence of interest by mass spectrometry.

Thus, considering this empirical approach used for MCPs separation from peptide hydrolysate, chromatography purification is time consuming and expensive. In this context, the chromatography modeling and simulation is an alternative to predict the separation of MCPs from hydrolysate in IMAC; this would reduce the number of experiments to be carried out, save time, and reduce the cost of purchasing expensive reagents. To predict chromatographic separations of MCP in IMAC, models such as the transport dispersive model must be developed to simulate the concentration profiles at the outlet of chromatography columns; yet, these models need input data [13]. A key piece of input data concerns adsorption isotherm, which gives information about the equilibrium between the solute quantity adsorbed on the solid phase and the concentration of the solute in the mobile phase, and numerous methods, such as adsorption-desorption, frontal analysis, perturbation, etc., are used for measuring adsorption isotherms [14,15]. Some of these methods for determining a sorption isotherm require a large quantity of product (e.g., frontal analysis) and in some cases, as for example the development of separation methods for MCPs in hydrolysate, very little product is available. Therefore, a major challenge is to develop methods able to determine isotherms while consuming very little product. These methods are notably based on the use of biosensors such as Surface Plasmon Resonance. Thus, SPR could be a good option since it requires very few peptides or hydrolysates and presents some similarities with IMAC; indeed, both techniques are based on the peptide-metal ion interactions [16]. In addition, SPR has been reported to be an efficient technique to screen MCPs in hydrolysates.

Therefore, the objective of this work was to determine IMAC adsorption isotherm parameters from SPR measurements in order to be able to further predict MCPs separation from hydrolysate. To our knowledge, this approach has not been studied except for a proof of concept that was previously carried out on small peptides (mainly di and tripeptide) using very low volume and concentration injections in our group [17]. In order to extend this approach, the present work is based on the study of a larger number of peptides and operating conditions for the injections. A pool of peptides constituted of 3 to 10 amino-acid residues were used to develop an efficient approach to predict each of the parameters of the isotherm in IMAC from their affinity parameters previously determined in SPR. Multiple operating conditions were simulated, on the one hand by carrying out injections over a wide range of concentrations and volumes, including conditions leading to overloaded elution profiles, and on the other hand by carrying out the elution in the isocratic mode or in the eluent gradient mode using imidazole. Indeed, imidazole was chosen as an eluent because it is a competitive agent commonly used in IMAC, which has a high affinity for immobilized metal ions compared to peptides. The relevance of the parameters was assessed based on the comparison of experimental elution profiles obtained from IMAC experiments and simulated elution profiles obtained using IMAC isotherm parameters predicted by different approaches.

2. Materials and Methods

2.1. Simulation Program

2.1.1. Axially Dispersed Plug Flow Model

The chromatography column was modeled by the axial-dispersed plug flow model. This transport dispersive model describes the mass transfer inside the column, taking into

Processes 2024, 12, 592 3 of 19

> consideration the isothermal adsorption, the radial homogeneity, the lumped coefficient for axial dispersion, and the mass transfer resistances [13].

> Thus, the mass balance was established considering that, for each slice of column, the Input is equal to the sum of Output plus Accumulation [18] and is defined below in Equation (1):

$$\begin{bmatrix} FC_i - S\varepsilon_T D_L \frac{\partial C_i}{\partial z} \end{bmatrix}_z = \begin{bmatrix} FC_i - S\varepsilon_T D_L \frac{\partial C_i}{\partial z} \end{bmatrix}_{z+\Delta z} + \frac{\partial}{\partial t} [S\Delta z (\varepsilon_T C_i + (1-\varepsilon_T)q_i)] \\
\text{Input} = \text{output} + \text{accumulation}$$
(1)

where F is the flow rate of the feed, C_i is the concentration of the peptide i in the mobile phase (g·L_{mobile phase}⁻¹), S is the section of the column, ε_T is the uniform porosity, D_L is the apparent axial dispersion coefficient (m²·s⁻¹), z is the axial coordinate (m), Δz is a differential slice of thickness, t is the time coordinate (s), q_i is the concentration of the peptide i at a given point in the stationary phase (g·L $^{-1}$). After simplification, the mass balance led to Equation (2):

$$\frac{\partial C_i}{\partial t} + \frac{1 - \varepsilon_T}{\varepsilon_T} \frac{\partial q_i}{\partial t} + \frac{u_s}{\varepsilon_T} \frac{\partial C_i}{\partial z} = D_L \frac{\partial^2 C_i}{\partial z^2} \quad \forall i = 1, 2, \dots, N_c \text{ and } z \in (0, L)$$
 (2)

where

 $\frac{\partial C_i}{\partial f}$ describes the accumulation in the mobile phase, $\frac{1-\epsilon_T}{\epsilon_T}$ represents V_s/V_m , which is the phase ratio, where V_s and V_m are the volumes of the stationary phase and mobile phase, respectively,

 $\frac{1-\varepsilon_T}{\varepsilon_T} \frac{\partial q_i}{\partial t}$ is the accumulation in the stationary phase, $\frac{u_s}{\varepsilon_T} \frac{\partial C_i}{\partial z}$ is the convective transport in the mobile phase,

 $D_L \frac{\partial^2 C_i}{\partial z^2}$ is the transport by axial dispersion in the mobile phase.

And where t is the time coordinate (s), z is the axial coordinate (m), ε_T is the total porosity of the column, u_s is the superficial velocity (m·s⁻¹), D_L is the apparent axial dispersion coefficient (m²·s⁻¹), N_c is the number of components in the system and L is the column length (m).

The accumulation term in the stationary phase can be expressed by a simplified Linear Driving Force-type relationship as the rate-limiting step of the process was considered to be the internal mass transfer:

$$\frac{\partial q_i}{\partial t} = k_m (q_i^* - q_i) \tag{3}$$

where k_m is the lumped mass transfer coefficient (s⁻¹), q_i is the concentration of the peptides at a given point in the stationary phase $(g \cdot L^{-1})$, t is the time (s), q_i^* is the peptide concentration in the stationary phase at equilibrium as defined by the Langmuir adsorption isotherm $(g \cdot L^{-1})$ in the next section.

2.1.2. Adsorption Isotherm

The adsorption isotherm represents the amount of peptides (noted q_i) adsorbed onto the stationary phase when thermodynamic equilibrium is reached, as a function of the concentrations of peptides present in the mobile phase (noted C_i) at constant temperature. The Langmuir isotherm was considered in this study [18], and for a single-component system, it is expressed by Equation (4):

$$q_i = \frac{q_{max,i} K_{A,i} C_i}{1 + K_{A,i} C_i} \tag{4}$$

Processes **2024**, 12, 592 4 of 19

In the case of a multi-component system, where other peptides or eluants like imidazole are involved, a competition effect must be taken into account and the Langmuir isotherm is expressed by Equation (5) [14]:

$$q_{i} = \frac{q_{max,i} K_{A,i} C_{i}}{1 + \sum_{j=1,n} K_{A,j} C_{j}}$$
 (5)

where i and j are components, n is the number of components in the system, $q_{max,i}$ is the maximal adsorption capacity of a peptide i (g·L_{stationary phase} $^{-1}$), q_i is the concentration of the peptide i in the stationary phase (g·L $^{-1}$), $K_{A,i}$ is the affinity constant (L·g $^{-1}$), C_i is the concentration of the peptide i in the mobile phase (g·L_{mobile phase} $^{-1}$).

Determining the isotherm parameters $q_{max,i}$ and $K_{A,i}$ is, therefore, essential for chromatography modeling and simulation.

2.1.3. Initial and Boundaries Conditions for Solving the Transport Dispersive Model and Other Parameters for Chromatography Modeling

To solve the equations with the *pdepe* solver of Matlab-R2020b, the initial conditions and boundary conditions must be established. First, the column was initially equilibrated by the loading buffer, leading to the initial peptide concentration at a given point z in the mobile and stationary phase equal to zero:

$$\begin{cases}
C(t = 0, z) = 0 \\
q(t = 0, z) = 0
\end{cases}$$
(6)

Secondly, the boundary conditions at the inlet of the column (z = 0) and at the outlet of the column (z = L) were as follows:

$$\begin{cases} \frac{\partial C}{\partial z} \Big|_{z=0} = \frac{u_s}{\varepsilon_T D_L} \times \left(C(t, z=0) - C_{feed}(t) \right) \\ \frac{\partial C}{\partial z} \Big|_{z=L} = 0 \end{cases}$$
 (7)

where t is the time coordinate (s), z is the axial coordinate (m), C is the concentration of the peptide in the mobile phase (g·L_{mobile phase}⁻¹), C_{feed} is the feed concentration of the peptide, q is the concentration of the peptide in the stationary phase (g·L⁻¹), ε_T is the total porosity of the column, u_s is the superficial velocity (m·s⁻¹), D_L is the apparent axial dispersion coefficient (m²·s⁻¹), and L is the column length (m).

During the injection step, C_{feed} (t) corresponds to the concentration of the solution injected into the column. As the column flow rate is kept constant, the volume injected depends on the injection time.

During the elution step, C_{feed} (t) corresponds to the concentration of the eluent over time. The eluent chosen here was imidazole. Thus, in the case of the isocratic elution mode, the concentration of imidazole used during elution was constant.

Meanwhile, in the case of the gradient elution mode, the idea was to simulate the protocol used experimentally where elution was carried out using a linear gradient of imidazole, varying from 0 to 600 mM over 60 min. Since the experimental retention times of all peptides did not exceed 20 min, the simulated elution was done with a linear gradient of imidazole varying from 0 to 300 mM in 30 min in order to shorten the simulation time. The slope of this linear gradient of concentration in imidazole was implemented considering the molecular weight of the eluent MW_{eluent} (g·mol⁻¹), and is given by Equation (8):

$$\frac{\Delta C}{\Delta t} = \frac{0.6-0}{60} \times MW_{eluent} = \frac{0.3-0}{30} \times MW_{eluent} = 0.01 \times MW_{eluent} \left(g \cdot L^{-1} \cdot min^{-1} \right)$$
(8)

All the other parameters concerning column dimensions (length, diameter, volume), volume and concentration of the peptide, eluent (imidazole) concentration, etc., were selected and entered in the model, as summarized in Table 1 as standard conditions.

Processes **2024**, 12, 592 5 of 19

Parameter (Unit)	Standard Conditions	Variation Range	Justification				
Injected peptide volume (μL)	50	10 to 50	1–5% of total column volume				
Peptide concentration (mM)	2 or 20	0.001 to 20	2 mM in IMAC experiments				
Peptide molecular weight (g/mol)	Peptide MW	280 to 1400	Average MW of a 2 to 10 residues peptide				
	0 mM isocratic	10 to 50 1–5% of total column volume 0.001 to 20 2 mM in IMAC experiments Average MW of a 2 to 10 residues peptide 0 to 500 mM in isocratic					
Imidazole concentration (mM)	Elution gradient: 0–600 mM in 60 min	-					
Flow rate (mL/min)	1	0.5 to 1.5	1 mL in IMAC experiments				
Total porosity (no unit)	0.48	0 to 1	0.48 in IMAC experiments				
Column volume (mL)	1	1 and 5	IMAC column dimensions				
Column diameter (cm)	0.7	-	-				
Column height (cm)	2.5	-	-				
Lumped mass transfer coefficient (Km) (min ⁻¹)	1×10^{-6}	-	-				
Apparent axial dispersion coefficient (D_L) (cm ² ·S ⁻¹)	0.05	-	-				

30

Simulation time (min)

Table 1. Parameters used in the simulation: standard conditions and variation range for studying the effect of each parameter in isocratic elution mode.

2.1.4. Study of the Concentration Profiles Obtained at the Column Outlet in the Case of Injections of Variable Concentration and/or Volume

In the case of low concentration and low volume injection of a peptide, the number of moles injected into the column was low and the dilution effect of the eluent led to low peptide concentration levels in the column. For low peptide concentrations, Equation (4) led to the following:

$$\lim_{C \to 0} q = q_{max} K_A C \tag{9}$$

where the product K_A*q_{max} corresponds to the slope of the Langmuir isotherm for small peptide concentrations in the mobile phase C. A similar result could be obtained in the case of a multi-component system (Equation (5)) if the concentrations of all the species present are sufficiently low. These conditions correspond to the domain of linearity of the isotherms and there is no longer any effect of competition between the species present. In the case of these low peptide concentrations, a rearrangement of Equation (2) and Equation (9) makes it possible to determine a velocity for each specie, which does not depend on its concentration; therefore, the theoretical retention time ($t_{R,theo}$) in a column of length L is expressed by Equation (10):

$$t_{R,theo} = \frac{L}{u} \left(1 + \frac{1 - \varepsilon_T}{\varepsilon_T} \frac{dq}{dC} \right) = \frac{L}{u} \left(1 + \frac{1 - \varepsilon_T}{\varepsilon_T} K_A q_{max} \right) ; \quad u = \frac{Q}{S\varepsilon_T}$$
 (10)

where u is the interstitial velocity of the mobile phase (m·s⁻¹), ε_T is the total porosity (without unit), L is the column length (m). The term dq/dC corresponds to the slope of the sorption isotherm at low peptide concentration (linearity zone), which is equal to $K_A * q_{max}$.

The injection of a small volume and low concentrations of each peptide results in symmetrical peaks at the column outlet, the retention time of each species being given by Equation (10). Analytical chromatography injections generally correspond to this case, with symmetrical peaks and retention times characteristic of each species. According to Equation (10), the experimental determination of the retention time t_R can then provide

Processes **2024**, 12, 592 6 of 19

information on the slope of the isotherm at the origin and thus, in the case of a Langmuir isotherm, determine the product $K_A * q_{max}$.

In the case of an injection of greater volume and/or higher concentration of a peptide, commonly known as column overload, some of the concentrations are no longer in the domain of linearity and the previous simplifications can no longer be carried out. The velocity of the specie then depends on the local concentration of that specie and of other species. Approaches have been developed to express these velocities within the framework of equilibrium theory [13]. In the case of a Langmuir isotherm for a single-component system (Equation (4)), the slope dq/dC of the isotherm decreases as the peptide concentration increases, which leads to the fact that the greater the concentration of the species, the greater the velocity in the column. An overload injection of peptide produces a dissymmetric peak with a tail behind the peak; thus, the time taken for the peak to reach its maximum depends on the concentrations involved.

Yet, for facilitating the reading of this manuscript, a single notation retention time (t_R) will be used to designate the time corresponding to the maximum of the peak. When the concentrations involved are low enough to remain within the range of linearity, this t_R corresponds to the theoretical retention time $t_{R,theo}$ given by Equation (10).

- 2.2. Adaptation of Affinity Constant K_A and Maximum Response R_{max} Obtained in SPR for Peptide Concentration Profile Simulation in IMAC
- 2.2.1. Peptides Investigated and Their Initial Binding Parameters Used for Initial Simulation

Investigated peptides were selected for their good/medium affinity for Ni²⁺ in the range of concentration studied according to SPR. Some of the peptides are potentially present in pea proteins [19] and potato proteins, and some in unknown sources of protein [17]; they are presented in Table 2.

In order to simulate the concentration profiles of peptides at the column outlet, input data (q_{max} ; $K_{A,IMAC}$ ($L \cdot g^{-1}$)) of peptides and imidazole were initially calculated from data obtained by SPR ($R_{max,SPR}$; $K_{A,SPR}$) and summarized in Table 2. Indeed, the conversion of $K_{A,SPR}$ (M^{-1}) into $K_{A,IMAC}$ ($L \cdot g^{-1}$) using the molecular weight MW ($g \cdot mol^{-1}$) of the peptide studied was given by the following equation:

$$K_{A,IMAC} = \frac{K_{A,SPR}}{MW} \tag{11}$$

Note that according to the Biacore[®] NTA sensor chip specification, and considering the thickness of the chip, a response of 100 RU (Resonance Unit) represents an adsorbed molecule concentration of about 1 g·L⁻¹. Therefore, the value of $q_{max,SPR}$ was calculated as follows:

$$q_{max,SPR} = \frac{R_{max,SPR}}{100} \tag{12}$$

where $q_{max,SPR}$ is the maximum adsorption capacity of peptides at the NTA sensor chip interface (g·L⁻¹) and R_{max} is the maximal resonance (RU) of peptides determined in SPR.

For the first simulations as described in the proof of concept published in [17], the following value was considered for the maximum capacity in IMAC: $q_{max,IMAC} = q_{max,SPR} = q_{max}$.

Therefore, within the simulation program, the peptide molecular weight MW (g·mol⁻¹), its affinity constant K_A (L·g⁻¹), and its maximum capacity q_{max} (g·L⁻¹) were entered to generate a chromatogram where the retention time ($t_{R,simulated}$, $t_{R,sim.}$) was read on the maximum of the peak.

Processes **2024**, 12, 592 7 of 19

Table 2. Pepti	ides investigated	and their corres	ponding input	data obtained	from SPR.
			D 0-1-1-1-0		

Source	No	Peptide	MW (g/mol)	$K_{A,SPR}$ (M ⁻¹)	R_{max}	$q_{max,SPR} \ { m g}\cdot { m L}^{-1}$	$K_{A,IMAC}$ $L \cdot g^{-1}$	$q_{max,IMAC} ext{g} \cdot ext{L}^{-1}$	K_A*q_{max}
	1	GRHRQKHS	1005.12	53,590.6	28.70	0.29	53.32	0.29	15.30
50	2	KGKSR	574.67	21,929.8	24.90	0.25	38.16	0.25	9.50
	3	НННННН	840.87	1,472,754.1	43.80	0.44	12.81	0.44	5.61
	4	KRHGEWRPS	1152.27	1355.2	366.30	3.66	1.18	3.66	4.32
pea proteins	5	HGSLHKNA	862.95	5115.1	72.38	0.72	5.93	0.72	4.29
ote	6	RHGEWRPS	1024.09	3290.6	81.30	0.81	3.21	0.81	2.61
pr	7	HGSLH	549.59	2928.3	38.40	0.38	5.33	0.38	2.05
ea	8	YPVGR	590.67	6385.7	15.00	0.15	10.81	0.15	1.62
<u>a</u>	9	QRHRK	723.90	1098.9	52.85	0.53	2.73	0.53	1.44
	10	GLH	325.36	638.2	19.30	0.19	1.96	0.19	0.38
	11	GLHLPS	622.71	179.0	54.50	0.55	0.29	0.55	0.16
	12	KERESH	784.82	206.8	76.90	0.85	0.14	0.85	0.12
	13	THTAQETAK	986.04	65,574.0	13.00	0.13	66.50	0.13	8.65
potato proteins	14	ASH	313.31	16,003.0	14.60	0.15	51.08	0.15	7.46
ot ot	15	DHGPKIFEPS	1126.22	12,900.0	15.50	0.16	11.45	0.16	1.77
rd Id	16	DNHETYE	906.85	682.0	16.10	0.16	0.75	0.16	0.12
	17	ННН	429.43	14,400.0	99.78	1.00	33.53	1.00	33.46
	18	HW	341.36	8850.0	109.90	1.10	25.93	1.10	28.50
	19	HGH	349.35	4310.0	93.70	0.94	12.34	0.94	11.56
	20	GNH	326.31	175.0	127.10	1.27	0.54	1.27	0.69
E	21	CAH	329.38	370.0	51.81	0.52	1.12	0.52	0.58
unkown	22	DAH	341.32	286.0	58.76	0.59	0.84	0.59	0.49
ş	23	DTH	371.35	370.0	41.20	0.41	1.00	0.41	0.41
ã	24	RTH	412.44	161.0	95.34	0.95	0.39	0.95	0.37
	25	NCS	322.34	483.0	23.59	0.24	1.50	0.24	0.35
	26	DSH	357.32	179.0	39.90	0.40	0.50	0.40	0.20
	27	EAH	355.35	169.0	28.54	0.29	0.48	0.29	0.14
		Imidazole	68.07	160.0	41.35	0.41	2.35	0.41	0.96

2.2.2. Adjustment of $q_{max,IMAC}$ Values to Improve Simulation of Peptides' Concentration Profiles in IMAC

2.2.2.1. Determination of a Correction Factor Applied to q_{max} of Each Peptide

An assumption made in the following was that the affinity of peptides for immobilized Ni²⁺ metal ions was similar in IMAC and SPR. The value of K_A (L·g⁻¹) was therefore kept constant for all simulations.

Due to the geometry difference between the IMAC column phase and SPR NTA-chip, and the difference in quantity of Ni²⁺ metal ions available on each support, it seems reasonable to assume that the value of $q_{max,IMAC}$ is different from that of $q_{max,SPR}$. The aim is therefore to determine a method that best estimates the value of $q_{max,IMAC}$ from that of $q_{max,SPR}$.

Thus, in order to study the influence of the nature of the stationary phase and also the properties of the peptide, in particular steric hindrance effects, a correction factor was first estimated for each peptide on $q_{max,SPR}$. For that purpose, several values of the correction factor were tested until the difference between the simulated and the experimental retention times was as minimal as possible. Since experimental elution was carried out in the presence of imidazole, the simulation had to take into account the multi-component isotherms (Equation (5)) of the peptide studied and the imidazole. Thus, in this first approach, the correction factor estimated for each peptide was also applied to the eluent (imidazole) at the same time.

Processes **2024**, 12, 592 8 of 19

2.2.2.2. Determination of a Mean Correction Factor Applied to Peptide q_{max}

From the various correction factors specific to each investigated peptide, a mean value was determined for the correction factor and applied to all peptides and eluent (imidazole) in order to determine the simulated retention times associated with it and to simplify the approach for further simulation of peptides in the mixture.

On the other hand, a study was made to determine whether the addition of such a mean correction factor had any impact on the linearity domain of the sorption isotherm for each peptide. To do so, the adsorption isotherms (Equation (4)) were plotted taking into account the average value of the correction factors for each peptide in such a way as to scan a large range of concentrations, especially at low concentrations. The study of the linearity range of each peptide already studied in the isocratic mode was used as a reference.

Moreover, a parametric sensitivity analysis was performed around this average correction factor to determine if better predictions could be obtained by slightly increasing or decreasing the value of this coefficient. This parametric sensitivity analysis was carried out by taking $\pm 2.5\%$, $\pm 5\%$, $\pm 10\%$, or $\pm 20\%$ of the mean value.

2.2.2.3. Experimental Measurement of the $q_{max,IMAC}$ of Imidazole and Determination of a New Correction Factor Applied to the q_{max} of Each Peptide

• Determination of a specific $q_{max,IMAC}$ for imidazole from experimental imidazole retention time

In this section, the affinity of peptides and imidazole for immobilized Ni²⁺ metal ions were still assumed to be the same in IMAC and SPR, thus K_A (L·g⁻¹) was not modified. Experimentally, measurements of the retention time of imidazole were performed at concentrations varying from 0.1 mM to 5000 mM imidazole, by injecting 50 μ L and eluting with PBS1X, pH 7.4 on both columns (which are described in Section 2.3). The value of $q_{max,IMAC}$ (g·L⁻¹) of imidazole was determined based on the expression of the theoretical retention time (Equation (10)). Theoretical retention time ($t_{R,theo}$) was taken as the mean of the imidazole experimental retention time corresponding to 0.1 mM and 1 mM imidazole concentrations only, i.e., low concentrations of imidazole in the linearity range of the sorption isotherm. Then, we checked if the set of values (experimental $q_{max,IMAC}$ imidazole, $K_{A,SPR}$ imidazole) could lead to simulated retention times closer to the experimental retention times of imidazole, even outside the linearity range of the sorption isotherm. This study could thus corroborate, in the case of imidazole, the hypothesis concerning the analogy of the K_A value between IMAC and SPR, and confirm the value of the maximum capacity of imidazole in the IMAC column ($q_{max,IMAC}$).

• Determination of a new correction factor specific to each peptide to be applied to q_{max} for each peptide

This study consisted in resuming the search for the correction factor to be applied for each peptide, but this time the experimental $q_{max,IMAC}$ for imidazole determined in the previous subsection was used immediately and there was no need to add a correction factor for imidazole since it was obtained by IMAC experiments. The simulation should then be even more reliable since the true $q_{max,IMAC}$ for imidazole was used. For selecting the correction factor for q_{max} of peptides, several values were tested and the value chosen is the one that minimizes the difference between the simulated retention time ($t_{R,sim}$) and experimental retention time (t_R).

The entire methodology used to adjust the values of $q_{max,IMAC}$ has been summarized graphically and is presented in Figure 1.

Processes **2024**, 12, 592 9 of 19

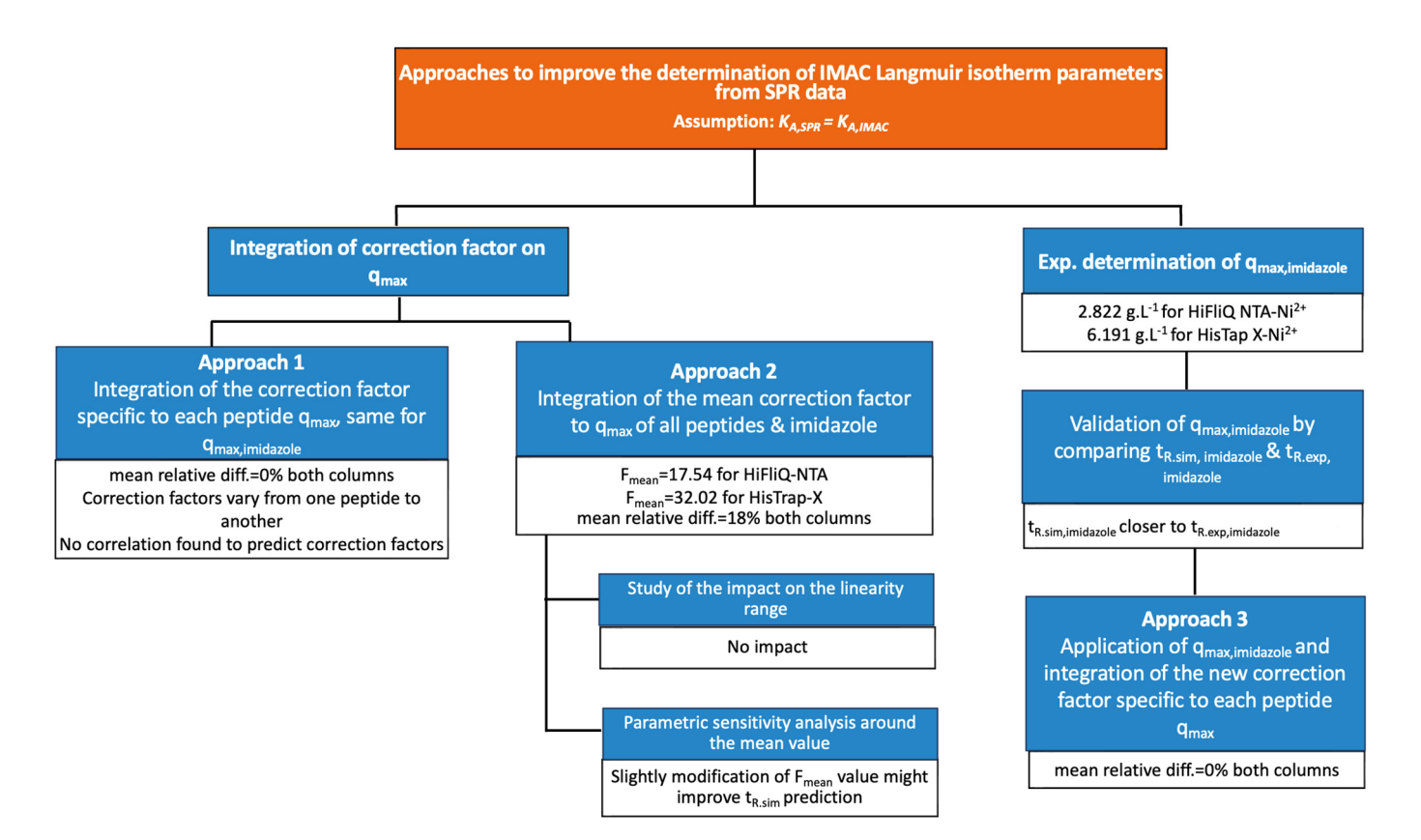


Figure 1. Approaches studied to improve the prediction of retention time during imidazole gradient elution mode.

2.3. Experimental IMAC Used to Evaluate the Validity of Peptides' Simulated Concentration Profiles

To determine experimentally the retention times of peptides in IMAC, two columns were used: HiFliQ-NTA and HisTrap-X. The complexing agent in HiFliQ-NTA was a tetradentate NTA, while the complexing agent was unknown (X) in the column HisTrap-X. Both columns were studied: HiFliQ-NTA was selected since it had the same complexing agent as the SPR chip, which might result in more reliable simulation; yet, peptides were more retained in the HisTrap-X column, which gives more data (experimental retention times, Table 3).

In this latter table, a horizontal line separates the first 7 peptides from the others, since they were the only ones retained during their passage in both IMAC columns. Thus, their results were more interesting to investigate. For better comparison, the dead time (0.72 min) through the pipes of the system was subtracted from the experimental retention time.

The standard IMAC protocol corresponded to the following operating conditions: 20 mM of peptide were loaded on HiFliQ-NTA and HisTrap-X columns using PBS1X buffer pH 7.4, and eluted using a gradient of imidazole (0–600 mM during 60 min) in order to obtain the experimental retention time as described in [19].

To compare experimental and simulated retention times, the measure of the absolute difference between the experimental retention time and the simulated retention time ($\Delta(t_{R,exp}-t_{R,sim})$) was carried out. The relative difference, showing the gap remaining between the simulated and the experimental retention times was expressed in percentage, and was calculated using Equation (13):

relative diff. =
$$\frac{absolute\ diff.}{t_{R,exp}} * 100 = \frac{\Delta(t_{R,exp} - t_{R,simu})}{t_{R,exp}} * 100$$
 (13)

Table 3. Various approaches used to improve the determination of IMAC Langmuir isotherm parameters from SPR data in order to simulate the peptides' concentration profiles in IMAC. The evaluation of each approach is based on the relative mean difference between $t_{R.exp}$ and $t_{R.sim}$. The lower it is, the closer $t_{R.exp}$ and $t_{R.sim}$. *Peptides not considered in all approaches due to their low affinities, ** peptides not considered in calculation of mean correction factor and mean relative difference for approach 2.

								Approach 1					Approach 2					Approach 3	3		
		Experimental IMAC		Initial Simulatio	on	Corre	ection Factor Fi	on <i>qmax</i> of Eac	h Peptide and Imid	azole	Mean co	rection Fmean F	actor on <i>qmax</i>	of Peptides and Im	idazole	Correction F		Each Peptide xperimental I!	, qmax Imidazole D MAC	etemined by	
No.	. Peptide	Peptide	^t R.exp (min)	t _{R.sim} (min)	$\Delta(t_{R.exp} - t_{R.sim}) \ (min)$	Relative Diff.	Correction Factor	qmax Corrected g·L ⁻¹	New ^t _{R.sim} (min)	Δ (tR exp $ t_{R.sim}$) (min)	Relative Diff.	Mean Correction Factor	qmax Corrected g·L ⁻¹	New ^t _{R.sim} (min)	$\Delta(t_{R.exp} - t_{R.sim})$ (min)	Relative Diff.	Correction Factor	qmax Corrected g·L ⁻¹	New t _{R.sim} (min)	$\Delta(t_{R.exp} - t_{R.sim})$ (min)	Relative Diff.
1	GRHRQKHS	15.28	0.480	14.800	97%	52.25	15.00	15.280	0.0×10^{00}	0%	32.02	9.19	9.985	5.30	35%	53.41	15.33	15.280	0.0 × 10 ⁰⁰	0%	
2	KGKSR **	4.18	0.485	3.695	88%	13.93	3.47	4.180	8.9×10^{-16}	0%	32.02	7.97	9.265	5.09	122%	13.85	3.45	4.181	1.0×10^{-03}	0%	
3	НННННН **	19.58	0.490	19.090	97%	132.85	58.19	19.580	3.6×10^{-15}	0%	32.02	14.02	7.625	11.96	61%	138.28	60.57	19.580	3.6×10^{-15}	0%	
4	KRHGEWRPS	8.38	0.675	7.705	92%	30.65	112.27	8.380	1.8×10^{-15}	0%	32.02	117.29	8.590	0.21	3%	31.74	116.26	8.380	1.8×10^{-15}	0%	
× 5	HGSLHKNA	6.88	0.500	6.380	93%	28.53	20.66	6.880	0.0×10^{00}	0%	32.02	23.18	7.450	0.57	8%	29.92	21.66	6.881	1.0×10^{-03}	0%	
d 6	RHGEWRPS	4.58	0.500	4.080	89%	21.97	17.86	4.580	0.0×10^{00}	0%	32.02	26.03	5.930	1.35	29%	23.51	19.11	4.580	0.0×10^{00}	0%	
Ls 7	HGSLH	4.68	0.495	4.185	89%	26.7	10.25	4.680	8.9×10^{-16}	0%	32.02	12.30	5.285	0.61	13%	29.87	11.47	4.680	8.9×10^{-16}	0%	
≖ 8	YPVGR *	0.48	0.485	0.005	1%	1	0.15	0.485	5.0×10^{-3}	1%	1.00	0.15	0.485	5.0×10^{-3}	1%	1.00	0.15	0.485	5.0×10^{-03}	1%	
9	QRHRK *	0.48	0.500	0.020	4%	1	0.53	0.495	1.5×10^{-2}	3%	1.00	0.53	0.495	1.5×10^{-2}	3%	1.00	0.53	0.495	1.5×10^{-02}	3%	
10	GLH *	3.28	0.495	2.785	85%	20.4	3.94	3.280	4.4×10^{-16}	0%	20.40	3.94	3.280	4.4×10^{-16}	0%	20.40	3.94	3.280	4.4×10^{-16}	0%	
11	GLHLPS *	3.28	0.500	2.780	85%	48.6	26.49	3.280	4.4×10^{-16}	0%	48.60	26.49	3.280	4.4×10^{-16}	0%	48.60	26.49	3.280	4.4×10^{-16}	0%	
12	KERESH *	0.48	0.500	0.020	4%	1	0.85	0.500	2.0×10^{-2}	4%	1.00	0.85	0.500	2.0×10^{-2}	4%	1.00	0.85	0.500	2.0×10^{-02}	4%	
	mean relative di	fference			92%					0%					18%					0%	
1	GRHRQKHS	8.38	0.480	7.900	94%	27	7.75	8.385	5.0×10^{-3}	0%	17.54	5.04	5.085	3.30	39%	27.53	7.90	8.383	3.0×10^{-03}	0%	
2	KGKSR **	0.48	0.485	0.005	1%	1	0.25	0.485	5.0×10^{-3}	1%	1.00	0.25	0.485	0.01	1%	1.00	0.25	0.485	5.0×10^{-03}	1%	
3	НННННН **	13.48	0.490	12.990	96%	72.5	31.76	13.485	5.0×10^{-3}	0%	17.54	7.68	4.625	8.86	66%	76.20	33.38	13.481	1.0×10^{-03}	0%	
4	KRHGEWRPS	5.18	0.675	4.505	87%	13.72	50.26	5.180	8.9×10^{-16}	0%	17.54	64.26	6.035	0.86	17%	14.31	52.42	5.180	8.9×10^{-16}	0%	
⊴ 5	HGSLHKNA	4.68	0.500	4.180	89%	16.9	12.24	4.675	5.0×10^{-3}	0%	17.54	12.70	4.815	0.14	3%	18.09	13.10	4.681	1.0×10^{-03}	0%	
E 6	RHGEWRPS	2.98	0.500	2.480	83%	12.5	10.16	2.975	5.0×10^{-3}	0%	17.54	14.26	3.885	0.90	30%	13.96	11.35	2.980	4.4×10^{-16}	0%	
Oilii 8	HGSLH	3.48	0.495	2.985	86%	17.6	6.76	3.480	4.4×10^{-16}	0%	17.54	6.74	3.470	0.01	0%	20.84	8.00	3.480	4.4×10^{-16}	0%	
₩ 8	YPVGR *	0.48	0.485	0.005	1%	1	0.15	0.485	5.0×10^{-3}	1%	1.00	0.15	0.485	5.0×10^{-3}	1%	1.00	0.15	0.485	5.0×10^{-03}	1%	
- 9	QRHRK *	0.48	0.500	0.020	4%	1	0.53	0.500	2.0×10^{-2}	4%	1.00	0.53	0.500	2.0×10^{-2}	4%	1.00	0.53	0.500	2.0×10^{-02}	4%	
10	GLH *	0.48	0.495	0.015	3%	1	0.19	0.495	1.5×10^{-2}	3%	1.00	0.19	0.495	1.5×10^{-2}	3%	1.00	0.19	0.495	1.5×10^{-02}	3%	
11	GLHLPS *	0.48	0.500	0.020	4%	1	0.55	0.500	2.0×10^{-2}	4%	1.00	0.55	0.500	2.0×10^{-2}	4%	1.00	0.55	0.500	2.0×10^{-02}	4%	
12	KERESH *	0.48	0.500	0.020	4%	1	0.85	0.500	2.0×10^{-2}	4%	1.00	0.85	0.500	2.0×10^{-2}	4%	1.00	0.85	0.500	2.0×10^{-02}	4%	
	mean relative di	fference			77%					0%					18%					0%	

Processes **2024**, 12, 592 11 of 19

The approach was validated when the relative difference was closer to zero, meaning the gap between simulated and experimental retention times was lower.

3. Results and Discussion

Two main parts will be developed in this section. The first part (Section 3.1) uses the simulation tool that has been developed to illustrate the influence of different parameters such as injected volume, injected peptide concentration, and imidazole concentration during isocratic elution. Throughout this first part, the simulations were carried out using Langmuir isotherm parameters calculated directly from the SPR data (Section 2.2.1).

The second part (Section 3.2) presents initial simulation with non-adjusted IMAC Langmuir parameters obtained in Section 2.2.1 and also presents improved simulation using the methodologies described in Section 2.2.2 to adjust Langmuir isotherm parameters. Simulation is carried out with imidazole gradient elution mode, which is closer to the IMAC experimental conditions.

3.1. Simulation of Peptide Concentration Profile in Isocratic Elution Mode: Effect of Various Parameters

3.1.1. Effect of Injected Volume of the Peptide

The effect of the injected volume onto the IMAC columns—which varied between 10 and 50 μ L—was investigated, while all the other parameters were kept constant. The 27 peptides listed in Table 2 were studied. Yet for clarity, we only presented trends obtained for some peptides in three main classes. The first class contains peptides GRHRQKHS, KGKSR, HHHHHHH, KRHGEWRPS, HGSLHKNA, RHGEWRPS, ASH, THTAQETAK, HHH, HW, and HGH, which have a good affinity for Ni²⁺. The simulated retention times were plotted as a function of the volume injected as illustrated in Figure 2A for the six peptides (i.e., GRHRQKHS, KGKSR, HHHHHHH, KRHGEWRPS, HGSLHKNA, and RHGEWRPS), and other results are given in the Supplementary Data (Figure S1A,B).

The results show that for the peptides having a good affinity for Ni²⁺, the simulated retention time decreases sharply when the injected volume increases (Figure 2A).

The second class contains some peptides (i.e., HGSLH, YPVGR, QRHRK, and DHG-PKIFEPS) that have medium affinity for Ni²⁺ and the same trend is observed although less pronounced (Figure S1C,D). Finally, the third class of peptides (i.e., GLH, GLHLPS, KERESH, DNHETYE, GNH, CAH, DAH, DTH, RTH, NCS, DSH, EAH) have very low affinity for Ni²⁺ ions and the retention time is not affected by the injected volume (Figure S1E). Whatever the class of peptide (whatever the affinity of peptide for Ni²⁺), when the injected volume increases (so the greater the moles of peptides injected), the curve tends to a plateau value, which is the residence time of peptides within the column ($t_{0,column} = 0.48$ min). In fact, the retention time of the peptides gets closer to this value when the injected volume increases and peptides just cross the column quickly.

3.1.2. Effect of the Peptide Concentration

The effect of peptide concentration on the retention time (t_R) was investigated between 0.001 and 20 mM. For better understanding, we first considered the HW peptide as an example for data interpretation.

Example of HW peptide

By performing the simulations at various peptide concentrations, we observed chromatogram deformations when the peptide concentration increased as illustrated in Figure 3.

For high concentrations of HW, at 20 mM and 8 mM (Figure 3A), the simulation generates oscillations, and the "peak" is not symmetrical at all. For the concentration of 2 mM, initial oscillations are lower, yet, the peak is still slightly asymmetrical (Figure 3B). Finally for lower concentrations, there are almost no more oscillations, and the simulated peak is well symmetrical (Figure 3C,D, obtained for 0.2 mM and 0.001 mM, respectively), meaning that the field of the linear chromatography domain is reached.

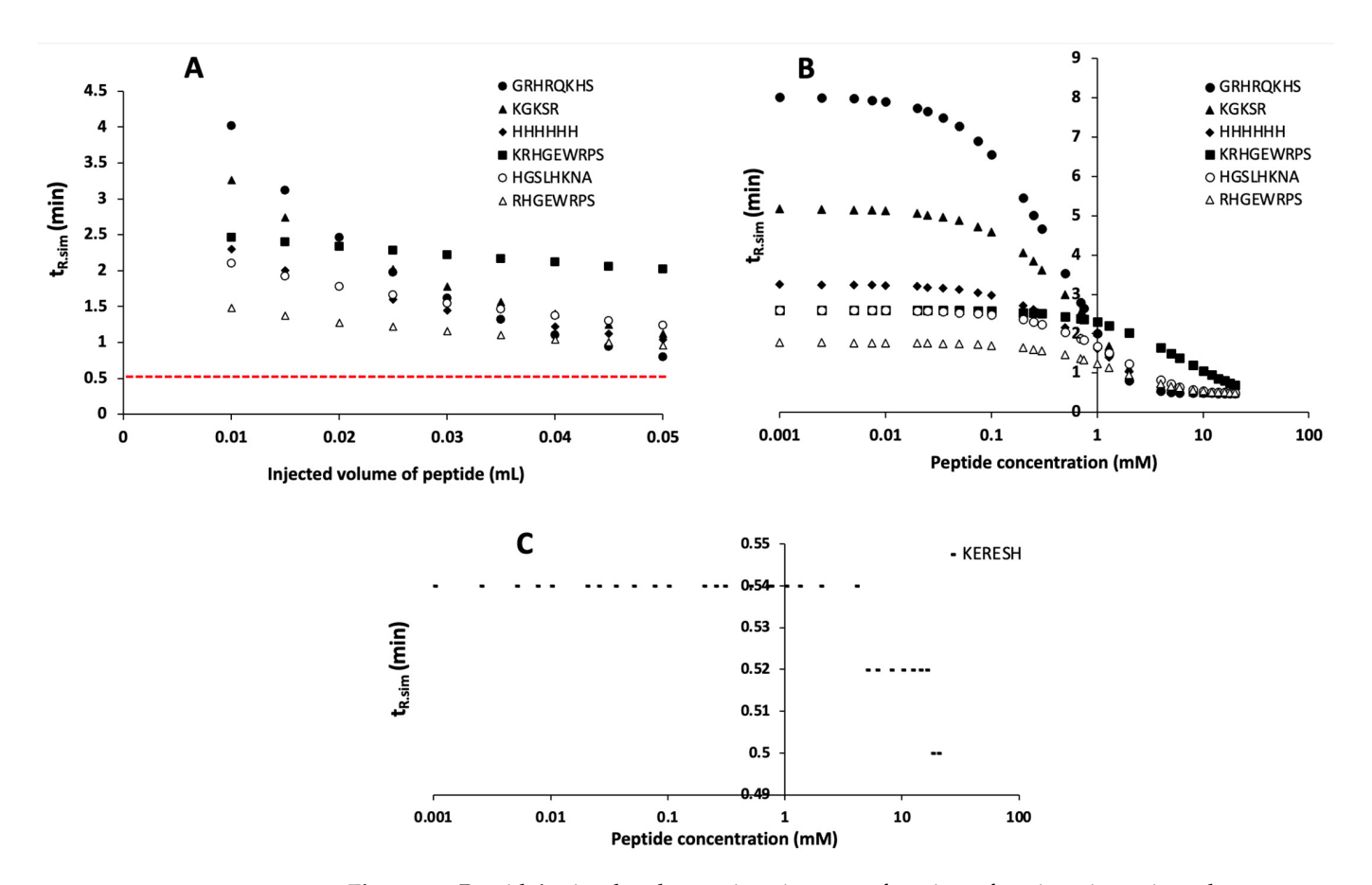


Figure 2. Peptide's simulated retention time as a function of various investigated parameters. **(A)** Peptide injected volume. **(B)** Peptide concentration for those having a high affinity for Ni²⁺. **(C)** Peptide concentration for those having a low affinity for Ni²⁺.

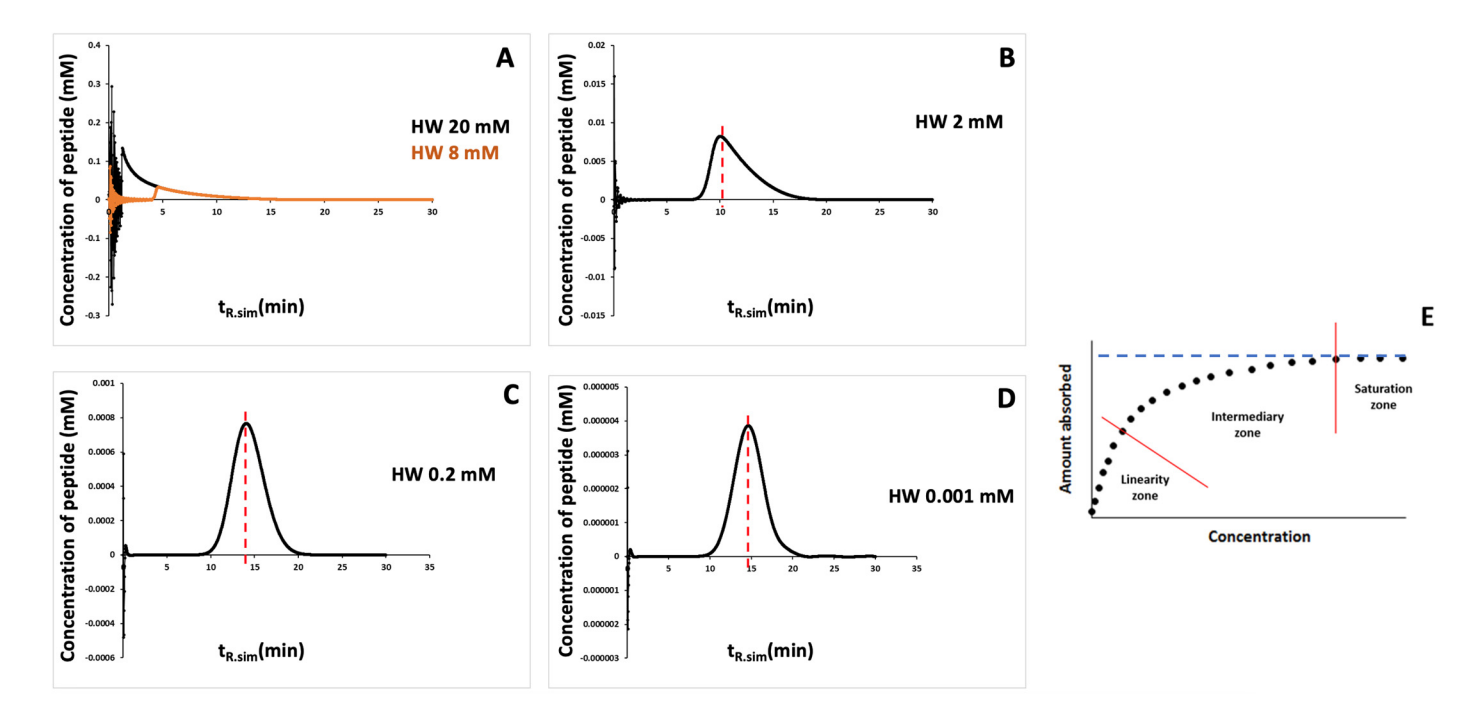


Figure 3. Simulated retention time ($t_{R.sim}$) versus concentration of the peptide HW (**A**) 8, 20 mM; (**B**) 2 mM; (**C**) 0.2 mM; (**D**) 0.001 mM), (**E**) linearity zone of sorption isotherm.

Therefore, there is a limit value of concentration from which the peak is no longer symmetrical, meaning that the obtained chromatogram is no longer in the field of linear chromatography [20,21], and thus, no longer in the linearity zone of the sorption isotherm (Figure 3E). There is also a so-called saturation zone, which corresponds to the plateau zone of the isotherm. Thus, while simulating the effect of concentration on the chromatogram obtained, we determined for each investigated peptide a sorption isotherm from which three zones were determined: linear, intermediary, and saturation zone.

• Determination of the saturation range and linearity range of concentration

Based on the expression presented in Equation (10), the retention time (t_R) depends directly on the slope of the sorption isotherm $\frac{dq}{dC}$ at low peptide concentration, which is a constant, equal to $K_{A,IMAC} * q_{max}$ in the linearity zone of the isotherm [17]. In the linear zone of the isotherm (Figure 3E), the retention time does not depend on the concentration of peptide injected. In the intermediary zone of the sorption isotherm (Figure 3E), the slope of the sorption isotherm is very sensitive to the peptide concentration, and so is the retention time. The plot of the simulated retention time as a function of the GRHRQKHS and other peptide concentrations is shown in Figure 2B. The retention time is constant in two areas corresponding to low and high concentrations, respectively. That means that the slope of the isotherm of GRHRQKHS is constant in the linear domain (i.e., low peptide concentration), then varies appreciably in the curved domain before reaching an asymptote in the zone of the isotherm plateau (i.e., high peptide concentration where saturation phenomenon is observed). In Figure 4, the GRHRQKHS peptide is shown as one of the peptides with the highest affinity for Ni²⁺, while for the KERESH peptide (one with the lowest affinity for Ni²⁺ in SPR), the retention time plot is concentration-independent (Figure 2C). For this latter KERESH peptide, the retention time does not vary significantly as a function of the peptide concentration. Indeed, the affinity of KERESH for Ni²⁺ is low, and the peptide is not retained upon simulation (low $t_{R,sim}$); thus, we cannot determine if the peptide is in its linearity or saturation zone at such investigated concentrations. Whatever the peptide sequence, the graphics presenting the simulated retention time $t_{R,sim}$, as a function of the peptide concentration are presented (Figure S2). From these graphics, we determined the linearity range and the saturation range for each investigated peptide (Table S1). The peptides for which neither the linearity zone nor the saturation zone can be determined are those with the lowest affinity for Ni²⁺. Indeed, whatever the amount of peptide injected, the peptide is not retained and these results can be related to the $K_A * q_{max}$ value of each peptide as shown in Figure 4. This figure shows that the peptides with high affinity for Ni²⁺ (i.e., GRHRQKHS, KGKSR, HHHHHHH, ASH, THTAQETAK, HHH, HW, and HGH) have a high $K_A * q_{max}$ product.

3.1.3. Effect of Imidazole Concentration

Initially, the imidazole concentration was studied in the isocratic mode, i.e., at constant concentration set between 0 to 500 mM, and for a peptide concentration of 2 mM, corresponding to the saturation zone of the sorption isotherm. While increasing the imidazole concentration (0–500 mM), the $t_{R.sim}$ decreases slowly. The peptides with the highest affinity for Ni²⁺ according to SPR data were quickly eluted, even in the absence of imidazole since there were not enough Ni²⁺ sites to bind the peptides at 2 mM, already close to the saturation zone (Figure S3A). The simulation on the peptides with the lowest affinity for Ni²⁺ determined in SPR (i.e., GNH, CAH, DAH, DTH, GLH, RTH, NCS, DSH, GLHLPS, EAH, KERESH, DNHETYE) proved to be the worst, with very low retention times close to the residence time already (0.48 min) observed from 50 mM of imidazole.

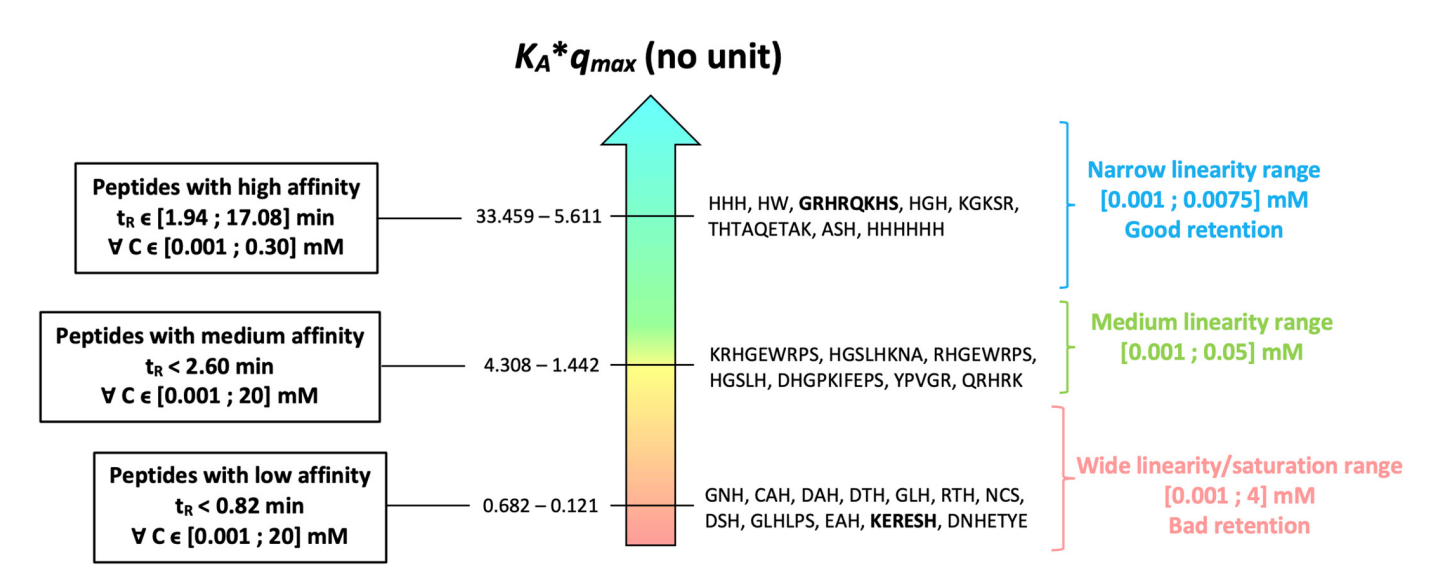


Figure 4. Effect of peptide concentration on linearity zone of its sorption isotherm and the link with the slope of the sorption isotherm K_A*q_{max} and peptide affinity for Ni²⁺. GRHRQKHS and KERESH were highlighted in bold since they served as example for discussion.

Meanwhile, the imidazole concentration was investigated-still in the isocratic mode—between 0 and 300 mM for a peptide concentration of 0.001 mM (Figure S3B). Indeed, this latter peptide concentration value was determined in the linearity range of the sorption isotherm for peptides with good and medium affinity for Ni²⁺ (i.e., GRHRQKHS, KGKSR, HHHHHH, KRHGEWRPS, HGSLHKNA, RHGEWRPS, ASH, THTAQETAK, HHH, HW, HGH, HGSLH, YPVGR, QRHRK, and DHGPKIFEPS). Results show that the retention time of peptides significantly decreases when the imidazole concentration increases (e.g., peptides ASH and THTAQETAK). Generally, for a concentration determined in the saturation or linearity range, peptides are no longer retained beyond 100 mM of imidazole (Figure S3A,B), which means that their imidazole concentration required for elution (the so-called IMC) is below 100 mM. Experimentally in IMAC (20 mM peptide concentration, gradient elution mode 0-600 mM in 60 min), all the peptides were eluted with the concentration of imidazole (IMC) lower than 100 mM, except for peptides with very high affinity for Ni²⁺ such as HHHHHH and GRHRQKHS using the HisTrap-X column and only HHHHHH using the HiFliQ-NTA column [19]. Hence, our simulation results are in agreement with the literature on experimental data, which reports low or very low peptide experimental retention times in the presence of imidazole as eluent, which is suitable to elute peptides with very high affinities [22,23].

3.2. Simulation of Peptide Concentration Profile in Gradient Elution Mode 3.2.1. Initial Simulation

In order to simulate the concentration profiles at the column outlet, input data (q_{max} ; $K_{A,IMAC}$ (L·g⁻¹)) of peptides and imidazole were initially calculated from data obtained by SPR without applying any correction factor (Section 2.2.1). The IMAC data (experimental retention times, $t_{R,exp}$.), the simulation data (simulated retention times, $t_{R,sim}$), and the analysis of the results (absolute and relative differences) are presented in Table 3 for HisTrap-X and HiFliQ-NTA columns, respectively. To evaluate the approach, the absolute difference ($\Delta(t_{R,exp} - t_{R,simu})$) and relative difference (Equation (13)) were calculated for each investigated peptide and the mean of the relative difference was calculated for peptides with high affinity for Ni²⁺ (i.e., GRHRQKHS, KGKSR, HHHHHHH, KRHGEWRPS, HGSLHKNA, RHGEWRPS, HGSLH), for both columns. Note that the peptides GLH and GLHLPS were not considered for this latter calculation of the mean of the relative difference since they are only retained in the HisTrap column. Upon the initial simulation, the calculation of the relative difference mean value showed a wide gap between the simulated and the experimental

Processes **2024**, 12, 592 15 of 19

retention times using the imidazole gradient elution mode, with a mean value of 92% and 77% for HisTrap-X and HiFliQ-NTA columns, respectively. Therefore, the prediction at this stage on retention times made by the simulation is still very far from experimental values. Thus, we need to find a methodology to better estimate the parameters of the isotherm in IMAC from SPR data.

3.2.2. Simulation of Peptide Concentration Profile Using Adjusted $q_{max,IMAC}$

3.2.2.1. Integration of a Specific Correction Factor on q_{max} of Each Peptide and Imidazole

A first approach consists of evaluating a correction factor applied on the value of q_{max} (g·L⁻¹) for each peptide while keeping K_A (L·g⁻¹) constant since we assumed a similar affinity of the peptide for Ni²⁺ in the SPR and in the IMAC column. The introduction of this correction factor (named F) should allow the simulated retention time ($t_{R,sim}$) to better match the experimental retention time ($t_{R,exp}$.) for each investigated peptide. The simulation results are presented in Table 3 (Approach 1) for HiFliQ-NTA and HisTrap-X columns and only peptides with a retention time greater than the residence time of non-retained species (i.e., with a corrected experimental retention time > 0.48) were assigned a correction factor. The calculation of the relative difference mean value was based only on the first seven peptides (peptides numbered from 1 to 7) that were retained in both columns. Indeed, regarding the HisTrap-X column results, the two peptides GLH and GLHLPS were not considered in the exploitation and analysis of results, since the simulation provided elution profiles with double peaks. In this latter case, the determination of the simulated retention time was made more complex, creating an important variability in the value of the correction factor to apply.

The addition of a well-adjusted correction factor F_i allowed the simulated retention time to match perfectly the experimental retention time with an average value of the relative difference equal to 0% for both columns. This result is linked to the fact that, for each peptide, we can adjust one parameter, the correction factor F, to allow one parameter, the simulated reaction time ($t_{R,sim}$), to be as close as possible to the experimental retention time ($t_{R,exp}$). A drawback of this approach is the difficulty of using a predictive aspect to evaluate a correction factor for each peptide.

3.2.2.2. Integration of a Mean Correction Factor on q_{max} of All Peptides and Imidazole

The aim of this second approach was to investigate whether a unique correction factor could be used for correcting the q_{max} of all peptides. The advantage would be to simulate all peptides using the same correction factor, which would be more practical for its application on peptide hydrolysate. The calculation of the mean value of the correction factor on the q_{max} of peptides was based on five of the seven peptides with good affinity for Ni^{2+} (i.e., GRHRQKHS, KRHGEWRPS, HGSLHKNA, RHGEWRPS, HGSLH). Indeed, the correction factors associated with peptide KGKSR and peptide HHHHHHH were not included in this calculation since their values were too far from the other peptides. The results of the mean correction factor ($F_{mean} = 32.02$ and 17.54 for HisTrap-X and HifliQ-NTA columns, respectively) and new simulated retentions are summarized in Table 3 (Approach 2). The results obtained show that the average relative difference associated with retention times while using a mean correction factor F_{mean} on q_{max} is 18% for both columns, which is not negligible to obtain a reliable prediction; however, the orders of magnitude obtained can provide interesting estimations.

Meanwhile, a study was carried out to determine whether the integration of such a mean correction factor F_{mean} on q_{max} of peptides (and applying the same value for imidazole) had any impact on the linearity zone of the sorption isotherm of peptides. To do so, the adsorption isotherms (defined by Equation (4)) were plotted (q vs. C) according to the calculation of q while applying the mean correction factor on q_{max} . The comparison with the linearity zone determined initially in the isocratic mode without the introduction of any correction factor was made. Results (Table S2) show that the use of the mean correction factor F_{mean} on the q_{max} of peptide and on imidazole has absolutely no impact on the

Processes **2024**, 12, 592 16 of 19

linearity range of the sorption isotherm of each peptide. Indeed, increasing the maximum capacity of q_{max} only impacts the proportion of peptides that will be adsorbed onto the stationary phase.

In addition, a study of the parametric sensitivity of the mean correction factor (F_{mean}) was conducted. The aim was to quantify the uncertainty associated with the mean correction factor (F_{mean}) by studying a range of possible values: $F_{mean} \pm 2.5\%$, $F_{mean} \pm 5\%$, $F_{mean} \pm 10\%$, and $F_{mean} \pm 20\%$. The results are summarized in Table S3 and show that increasing the value of the mean correction factor on q_{max} only increases the mean value of the relative difference between the simulated and the experimental retention time values. Inversely, decreasing the value of this mean correction factor F_{mean} slightly reduces the mean value of the relative difference. A value between 2.5% and 5% should be taken into consideration for the HiFliQ-NTA column, and a value around 10% for the HisTrap-X column. Thus, slightly correcting the value of the mean correction factor on q_{max} (i.e., 16.886 g·L⁻¹ and 28.818 g·L⁻¹ for HiFliQ-NTA and HisTrap-X columns, respectively) would slightly improve the prediction of the peptide's simulated retention time.

3.2.2.3. Evaluation of the Use of Experimental $q_{max,IMAC}$ of Imidazole Combined with the Integration of a New Correction Factor on q_{max} of Each Peptide

For the two previous approaches, the correction factor (F_i) applied to the q_{max} of the peptide was also applied to the q_{max} of imidazole as an eluent. Therefore, the aim of this third approach is to determine the q_{max} of imidazole experimentally in order to improve the accuracy of simulation. For this purpose, measurements of the retention time of imidazole in IMAC were performed for various concentrations (from 0.001 mM to 5000 mM) by eluting with PBS1X pH 7.4 only; retention times as a function of imidazole concentration are illustrated on Figure 5.

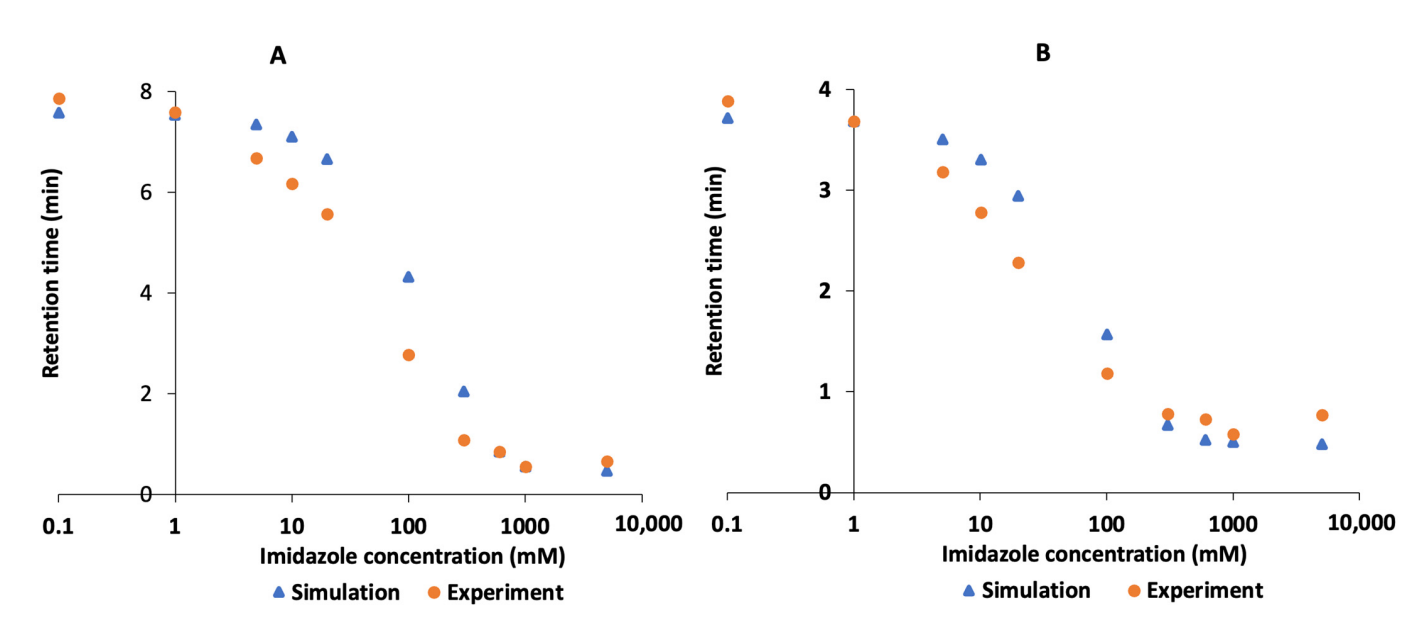


Figure 5. Imidazole simulated retention times with $q_{max,IMAC}$ and experimental retention times (**A**) for HisTrap-X and (**B**) for HiFliQ-NTA columns.

The calculations show that for q_{max} , IMAC is 6.191 g·L⁻¹ for the HisTrap-X column and 2.822 g·L⁻¹ for the HiFliQ-NTA column. These values were determined in the linearity zone of the sorption isotherm using Equation (10). To check the validity of the imidazole isotherm parameters determined, the simulation of retention time was run and compared to experimental values for specific concentrations. The results (Figure 5A,B for HisTrap-X and HiFliQ-NTA, respectively) show that simulated retention times of imidazole are fairly close to the expected experimental retention time of imidazole, even outside the linearity range of the sorption isotherm. For each column, the mean value of the relative difference

Processes **2024**, 12, 592 17 of 19

between the imidazole experimental retention time and imidazole simulated retention time illustrated in Figure 5A,B is, respectively, 15% (HiFliQ-NTA column) and 14% (HisTrap-X column) (Table S4), which remains relatively low.

It should be reminded that, for this approach (Approach 3), the imidazole K_A (L·g⁻¹) value used for the calculation of $q_{max,IMAC}$ from $t_{R,theo}$ as well as for IMAC simulations is the K_A (2.35 g·L⁻¹) value obtained from SPR. The good agreement between the simulated and the IMAC experimental retention times observed previously for a wide range of imidazole concentrations suggests that, the initial hypothesis concerning the K_A value, indicating that the affinity of a given peptide for immobilized Ni²⁺ does not change as a function of the technology used (IMAC or SPR), can be considered acceptable in the case of imidazole as well. This hypothesis requires further investigation to be truly confirmed in the case of peptides.

Then, the values of the maximum capacity of imidazole in the IMAC column $(q_{max,IMAC, imidazole})$ were applied to simulate the peptide retention times. For that purpose, the correction factor to be applied to the $q_{max,IMAC}$ for each peptide was estimated like in Section 2.2.2.1, but this time by also applying this experimental $q_{max,IMAC, imidazole}$ at the same time $(q_{max,IMAC, imidazole} = 2.822 \text{ g} \cdot \text{L}^{-1}$ and 6.191 g·L⁻¹ for HiFliQ and HisTrap columns, respectively). Results are summarized in Table 3 (Approach 3) and show that the average value of the relative difference is closer to 0% for both columns.

Regarding the comparison between the correction factors determined in Section 3.2.2.2 (same correction factor on q_{max} applied both for the peptide and imidazole) and the correction factors determined in this actual section (Section 3.2.2.3; correction factor on q_{max} specific for each peptide while using experimental $q_{max,IMAC, imidazole}$ specific for imidazole), the values remain in the same order of magnitude but are slightly better when the experimental $q_{max,IMAC, imidazole}$ is used.

4. Conclusions and Perspectives

The aim of the present work was to develop an approach to better understand how to predict each of the parameters of the sorption isotherm of peptides in IMAC ($q_{max,IMAC}$ and $K_{A,IMAC}$) from data obtained in SPR ($q_{max,SPR}$, $K_{A,SPR}$) in order to predict the separation of peptides in IMAC. Simulated retention times obtained using the parameters were compared to experimental retention times to evaluate the validity of prediction. A preliminary study, using directly the parameters obtained in SPR for IMAC, led to a huge difference between simulated and experimental retention times of peptides. We hypothesized that the limitations of this approach were due to the difference in geometry between the SPR sensor ship and the IMAC chromatographic phase. Several approaches have therefore been studied to find out how to take this into account and minimize the difference between experimental and simulated results. The most interesting one turned out to be the introduction of a correction factor justified by the geometry difference of the support in SPR and in IMAC on q_{max} alone. In the meantime, we assumed that the affinity of peptides for immobilized Ni²⁺ did not change depending on the technology used (SPR vs. IMAC), thus K_A was not modified by the introduction a correction factor.

The first approach, which is based on the calculation of a correction factor F_i to adjust the $q_{max,IMAC}$ of each peptide and imidazole eluent, provides a good match between the simulated and experimental retention times. One drawback, however, is that this approach does not provide a correlation to obtain the correction factors (Approach 1).

The second approach consists of applying a mean correction factor F_{mean} to the $q_{max,IMAC}$ of all peptides and imidazole. It led to relative errors in retention times of around 18% on average. Thus, the use of an average correction factor to evaluate IMAC capacities in relation to those measured in SPR is a global approach which provides orders of magnitude, but for which predictions will be less reliable than with individual measurements.

To improve prediction capabilities, a third approach was studied: the maximum capacity of imidazole was experimentally determined and applied while a correction factor,

Processes **2024**, 12, 592 18 of 19

estimated by minimising the difference between the experimental and simulated retention times, was applied to the q_{max} of each peptide. Although this procedure does not yet provide a global prediction method, the possibility of having specific values for the q_{max} of imidazole as well as for the q_{max} of each peptide studied provides an interesting basis for carrying out simulations.

A key assumption underlying these different approaches is that the affinity of the peptides and eluent for immobilized Ni^{2+} does not change according to the technology used (SPR vs. IMAC), and therefore that the K_A value is similar when switching from SPR to IMAC. Studies carried out over a wide concentration range for imidazole using two types of IMAC columns seem to have corroborated this hypothesis in the case of imidazole. Further studies will be carried out to fully confirm this hypothesis in the case of peptides.

Thus, if we refer to the initial objective—i.e., to determine the parameters of peptide IMAC isotherms from SPR data when very few quantities of peptides are available to carry out experiments—keeping the K_A value obtained in SPR for IMAC means that only one parameter, the q_{max} capacity value, needs to be identified for the isotherm, which can be done by minimizing the difference between the simulated and experimental retention times. Therefore, these results are promising and can help to predict MCPs separation in IMAC; further studies will be carried out to apply this approach on synthetic hydrolysates (mixture of synthetic peptides) and to real laboratory hydrolysates.

On the other hand, the effect of the parameters studied showed that, as expected for overload injections in the case of Langmuir isotherms, the retention time of the peptides decreases when the injected volume increases. Similarly, when the peptide concentration increases and is out of the linearity zone, simulation leads to asymmetric peaks. It is therefore important to choose the volumes and concentrations of these injections carefully in order to exploit either the $t_{R\ theo}$ value obtained in the linearity zone or, if desired, the information from overloaded concentration profiles.

Supplementary Materials: The following supporting information can be downloaded at: https://www.mdpi.com/article/10.3390/pr12030592/s1, Figure S1: Effect of the peptide injected volume on the retention time basing on classes of peptides; Figure S2. Effect of the concentration of peptide on retention time. The linearity zone of each peptide was determined and it corresponds to the zone where the retention time doesn't vary in function of the concentration; Figure S3. Simulated retention time versus imidazole concentration for ASH, THTAQETAK at 2mM (A) and 0.001 mM (B). Simulation was performed in isocratic elution mode; Table S1. Linearity and saturation zone determined from the previous graph; Table S2. Linearity zone before and after addition of the mean correction factor on q_{max} of peptides; Table S3. Parametric sensitivity analysis on the mean correction factor of q_{max} ; Table S4. Experimental and simulated retention times of imidazole for HisTrap-X and HiFliQ NTA columns. * Concentration not considered in the calculation of the mean relative difference.

Author Contributions: Conceptualization, R.I., L.M. and L.C.-R.; Methodology, L.M. and L.C.-R.; Formal analysis, R.I., P.J., A.M. and J.A.C.E.; Investigation, R.I., P.J., A.M. and J.A.C.E.; Writing—original draft, R.I., P.J. and A.M.; Writing—review & editing, L.M. and L.C.-R.; Supervision, L.M. and L.C.-R.; Project administration, L.C.-R.; Funding acquisition, L.C.-R. All authors have read and agreed to the published version of the manuscript.

Funding: This research was funded by French ministry government for the MESR grant, the ANR JCJC MELISSA (2020–2024), the "Impact Biomolecules" project of the "Lorraine Université d'Excellence" (Investissements d'avenir-ANR project number 15-004), and the project MELISSA ICEEL INTRA.

Data Availability Statement: Data are contained within the article.

Acknowledgments: The authors thank Mads BJØRLIE from Denmark Technical University for his contribution to the determination of SPR data of peptides potentially present in potato proteins.

Conflicts of Interest: The authors declare no conflict of interest.

References

1. Guo, L.; Harnedy, P.A.; Li, B.; Hou, H.; Zhang, Z.; Zhao, X.; FitzGerald, R.J. Food protein-derived chelating peptides: Biofunctional ingredients for dietary mineral bioavailability enhancement. *Trends Food Sci. Technol.* **2014**, *37*, 92–105. [CrossRef]

- 2. Hou, Y.; Wu, Z.; Dai, Z.; Wang, G.; Wu, G. Protein hydrolysates in animal nutrition: Industrial production, bioactive peptides, and functional significance. *J. Anim. Sci. Biotechnol.* **2017**, *8*, 24. [CrossRef] [PubMed]
- 3. Yesiltas, B.; García-Moreno, P.J.; Gregersen, S.; Olsen, T.H.; Jones, N.C.; Hoffmann, S.V.; Marcatili, P.; Overgaard, M.T.; Hansen, E.B.; Jacobsen, C. Antioxidant peptides derived from potato, seaweed, microbial and spinach proteins: Oxidative stability of 5% fish oil-in-water emulsions. *Food Chem.* **2022**, *385*, 132699. [CrossRef] [PubMed]
- 4. Udechukwu, M.C.; Collins, S.A.; Udenigwe, C.C. Prospects of enhancing dietary zinc bioavailability with food-derived zinc-chelating peptides. *Food Funct.* **2016**, *7*, 4137–4144. [CrossRef] [PubMed]
- 5. Wu, W.; Yang, Y.; Sun, N.; Bao, Z.; Lin, S. Food protein-derived iron-chelating peptides: The binding mode and promotive effects of iron bioavailability. *Food Res. Int.* **2020**, *131*, 108976. [CrossRef] [PubMed]
- 6. Guo, L.; Hou, H.; Li, B.; Zhang, Z.; Wang, S.; Zhao, X. Preparation, isolation and identification of iron-chelating peptides derived from Alaska pollock skin. *Process Biochem.* **2013**, *48*, 988–993. [CrossRef]
- 7. Lv, Y.; Liu, Q.; Bao, X.; Tang, W.; Yang, B.; Guo, S. Identification and Characteristics of Iron-Chelating Peptides from Soybean Protein Hydrolysates Using IMAC-Fe³⁺. *J. Agric. Food Chem.* **2009**, *57*, 4593–4597. [CrossRef] [PubMed]
- 8. Wang, C.; Li, B.; Ao, J. Separation and identification of zinc-chelating peptides from sesame protein hydrolysate using IMAC-Zn²⁺ and LC–MS/MS. *Food Chem.* **2012**, *134*, 1231–1238. [CrossRef] [PubMed]
- 9. Gutiérrez, R.; Martín Del Valle, E.M.; Galán, M.A. Immobilized Metal-Ion Affinity Chromatography: Status and Trends. *Sep. Purif. Rev.* **2007**, *36*, 71–111. [CrossRef]
- 10. Pearson, R.G. Hard and Soft Acids and Bases. J. Am. Chem. Soc. 1963, 85, 3533-3539. [CrossRef]
- 11. Becker, K.; Van Alstine, J.; Bülow, L. Multipurpose peptide tags for protein isolation. *J. Chromatogr. A* **2008**, 1202, 40–46. [CrossRef] [PubMed]
- 12. Ueda, E.K.M.; Gout, P.W.; Morganti, L. Current and prospective applications of metal ion–protein binding. *J. Chromatogr. A* **2003**, 988, 1–23. [CrossRef] [PubMed]
- 13. Guiochon, G.; Shirazi, D.G.; Felinger, A.; Katti, A.M. Fundamentals of Preparative and Nonlinear Chromatography, 2nd ed.; Academic Press: Boston, MA, USA, 2006; ISBN 978-0-12-370537-2.
- 14. Seidel-Morgenstern, A. Experimental determination of single solute and competitive adsorption isotherms. *J. Chromatogr. A* **2004**, 1037, 255–272. [CrossRef] [PubMed]
- 15. Lenz, K.; Beste, Y.A.; Arlt, W. Comparison of static and dynamic measurements of adsorption isotherms. *Sep. Sci. Technol.* **2002**, 37, 1611–1629. [CrossRef]
- 16. Irankunda, R.; Camaño Echavarría, J.A.; Paris, C.; Stefan, L.; Desobry, S.; Selmeczi, K.; Muhr, L.; Canabady-Rochelle, L. Metal-Chelating Peptides Separation Using Immobilized Metal Ion Affinity Chromatography: Experimental Methodology and Simulation. *Separations* **2022**, *9*, 370. [CrossRef]
- 17. Muhr, L.; Pontvianne, S.; Selmeczi, K.; Paris, C.; Boschi-Muller, S.; Canabady-Rochelle, L. Chromatographic separation simulation of metal-chelating peptides from surface plasmon resonance binding parameters. *J. Sep. Sci.* 2020, 43, 2031–2041. [CrossRef] [PubMed]
- 18. Carta, G.; Jungbauer, A. *Protein Chromatography: Process Development and Scale-Up*; Wiley-VCH: Weinheim, Germany, 2010; ISBN 978-3-527-31819-3.
- 19. Irankunda, R.; Camaño Echavarría, J.A.; Paris, C.; Selmeczi, K.; Stefan, L.; Boschi-Muller, S.; Muhr, L.; Canabady-Rochelle, L. Deciphering Interactions Involved in Immobilized Metal Ion Affinity Chromatography and Surface Plasmon Resonance for Validating the Analogy between Both Technologies. *Inorganics* **2024**, *12*, 31. [CrossRef]
- 20. Schmidt-Traub, H. (Ed.) Preparative Chromatography of Fine Chemicals and Pharmaceutical Agents; Wiley-VCH: Weinheim, Germany, 2005; ISBN 978-3-527-30643-5.
- 21. Sofer, G.K.; Hagel, L. *Handbook of Process Chromatography: A Guide to Optimization, Scale Up, and Validation*; Academic Press: San Diego, CA, USA, 1997; ISBN 978-0-12-654266-0.
- 22. Ren, D.; Penner, N.A.; Slentz, B.E.; Mirzaei, H.; Regnier, F. Evaluating Immobilized Metal Affinity Chromatography for the Selection of Histidine-Containing Peptides in Comparative Proteomics. *J. Proteome Res.* **2003**, *2*, 321–329. [CrossRef] [PubMed]
- 23. Ren, D.; Penner, N.A.; Slentz, B.E.; Regnier, F.E. Histidine-Rich Peptide Selection and Quantification in Targeted Proteomics. *J. Proteome Res.* **2004**, *3*, 37–45. [CrossRef]

Disclaimer/Publisher's Note: The statements, opinions and data contained in all publications are solely those of the individual author(s) and contributor(s) and not of MDPI and/or the editor(s). MDPI and/or the editor(s) disclaim responsibility for any injury to people or property resulting from any ideas, methods, instructions or products referred to in the content.